

1 **ORCHIDEE-SRC v1.0: an extension of the land surface**
2 **model ORCHIDEE for simulating short rotation coppice**
3 **poplar plantations**

4

5 T. De Groot^{1,2}, D. Zona^{1*}, L. S. Broeckx¹, M. S. Verlinden¹, S. Luysaert³, V. Bellassen⁴, N.
6 Vuichard³, R. Ceulemans¹, A. Gobin², I. A. Janssens¹

7

8 [1]{Research Group of Plant and Vegetation Ecology, Department of Biology, University of
9 Antwerp, Universiteitsplein 1, BE-2610 Wilrijk, Belgium}

10 [2]{Unit Environmental Modelling, VITO, Boeretang 200, B-2400 Mol, Belgium}

11 [3]{CEA-CNRS-UVSQ, UMR8212 – Laboratoire des sciences du climat et de
12 l'environnement (LSCE), Orme des Merisiers, F-91191 Gif-sur-Yvette, France}

13 [4]{CDC Climat, 47 rue de la Victoire, F-75009 Paris, France}

14 [*]{now at: Department of Animal and Plant Sciences, The University of Sheffield, Western
15 Bank, Sheffield S10 2TN, UK}

16

17 Correspondence to: T. De Groot (Toon.DeGroot@uantwerpen.be)

18

19 **Abstract**

20 Modelling biomass production and the environmental impact of short rotation coppice (SRC)
21 plantations is necessary for planning their deployment, as they are becoming increasingly
22 important for global energy production. This paper describes the modification of the widely
23 used land surface model ORCHIDEE for stand scale simulations of SRC plantations.

24 The model uses weather data, soil texture and species-specific parameters to predict the
25 aboveground (harvestable) biomass production, as well as carbon and energy fluxes of an
26 SRC plantation. Modification to the model were made to the management, growth, and
27 allocation modules of ORCHIDEE.

28 The modifications presented in this paper were evaluated using data from two Belgian, poplar
29 based SRC sites, for which multiple measurements and meteorological data was available.
30 Biomass yield data was collected from 23 other sites across Europe and compared to 22
31 simulations across a comparable geographic range. The simulations show that the model
32 performs very well to predict aboveground (harvestable) biomass production (within
33 measured ranges), ecosystem photosynthesis ($R^2 = 0.78$, NRMSE = 0.064, PCC = 0.89) and
34 ecosystem respiration ($R^2 = 0.95$, NRMSE = 0.078 PCC = 0.91). Also soil temperature and
35 soil moisture are simulated adequately, but due to the simplicity of the soil moisture
36 simulation, there are some discrepancies, which also influence the simulation of the latent
37 heat flux.

38 Overall, the extended model, ORCHIDEE-SRC, proved to be a tool suitable for predicting
39 biomass production of SRC plantations.

40

41 1 Introduction

42 In recent years, a great deal of research has gone into the development of renewable energy as
43 a way to sustain energy production without contributing to climate change. The Europe 2020
44 headline targets of the European Commission state that by 2020, greenhouse gas emissions
45 should be 20% lower than in 1990 and 20% of the European energy has to be renewable (EC,
46 2010). The National Renewable Energy Action Plan (NREAP) predicts that in Europe 34.3%
47 of the electricity production and 21.3% of the heating and cooling energy requirement will
48 come from renewable energy production by 2020 (Zervos et al., 2011). An important share of
49 this renewable energy production will come from biomass. Both annual and perennial energy
50 crops and biomass residues from agriculture, forestry and processing industries can be used.

51

52 SRC plantations are perennial energy crops with fast growing tree species, mostly poplar
53 (*Populus spp.*) or willow (*Salix spp.*), that are intensively managed in a coppice system
54 (Herve and Ceulemans, 1996; Aylott et al., 2008). The rotation duration typically ranges from
55 2 to 5 years. At the end of the rotation the shoots are cut back to the ground in winter and the
56 stumps resprout the next spring. The harvested wood is then dried and used for energy
57 production. Management intensity of a SRC plantation is thus higher than in traditional
58 forests, but less than in food crops (Hansen, 1991).

59

60 Because of the growing societal demand for energy from biomass, SRC plantations are likely
61 to become more widespread, although the full consequences on the carbon (C), water and
62 energy budgets are not yet fully understood. For this reason models are needed that can
63 simulate the larger-scale effects of wide-spread SRC use, which are sufficiently general to
64 allow application at larger scales, while being specific in the essential details.

65

66 The objective of this study is to further develop an existing land surface model called
67 ORCHIDEE, to have the model simulate the C and water fluxes of SRC plantations over a
68 range of site conditions. In the future we want to use this model to test a number of
69 management scenarios across Europe to study the variation in the management effects on
70 biomass production and CO₂ uptake. To this aim we made changes to the management,
71 growth and allocation modules of ORCHIDEE, adjusted the parameterization and evaluated

72 the performance of the adapted model against site-level information from two operationally
73 managed SRC stands in Belgium.

74

75 **2 Materials and methods**

76 **2.1 Model description**

77 ORCHIDEE is a mechanistic land surface model that was designed to operate from regional
78 to global scales. The model is composed of two components: (i) SECHIBA, which computes
79 the energy and hydrology budget on a half-hourly basis, and (ii) STOMATE, which simulates
80 the carbon cycle on a daily time scale. The equations used by ORCHIDEE are given in
81 Ducoudre et al. (1993), Krinner et al. (2005) and in the online documentation
82 (<http://forge.ipsl.jussieu.fr/orchidee>). The source code can be accessed at
83 http://forge.ipsl.jussieu.fr/orchidee/browser/tags/ORCHIDEE_1_9_5.

84

85 For these simulations, ORCHIDEE needs seven meteorological variables at a 30 min interval,
86 i.e.: wind speed, air pressure, short-wave radiation, long-wave radiation, air temperature,
87 precipitation and specific air humidity. Atmospheric CO₂ concentrations are required on a
88 yearly time scale and a representative soil texture for the site is sufficient.

89

90 We evaluated the modifications to ORCHIDEE using output variables that are related to the
91 carbon and energy balance, i.e.: Gross Primary Production (GPP), Net Ecosystem Exchange
92 (NEE), Net Primary Production (NPP), respiration (R), sensible heat (H) and latent heat (LE).

93

94 In version r512, the C in ORCHIDEE is distributed over three main pools: (i) biomass, (ii)
95 litter and (iii) soil carbon. These pools are divided into 8, 2 and 3 sub-pools, respectively. The
96 biomass pool consists of leaves, roots, above- and belowground sapwood, above- and
97 belowground heartwood, fruits (i.e. both flowers and fruits) and a carbohydrate reserve. The
98 litter pool is composed of a structural and a metabolic litter pool. The former contains high-
99 lignin litter, with a slow decay rate, while the latter contains low-lignin litter, which decays

100 faster. The soil carbon consists of a fast, a slow and a passive pool, corresponding to the time
101 it takes for the C in these pools to become biologically available again.

102

103 The soil water in r512 is simulated using two layers following the Choisnel scheme (Choisnel,
104 1977). The bottom layer is always present. The top layer is a dynamic layer that is absent in
105 drier periods, and is created when it starts raining. When the top layer fills with rain, the layer
106 expands as the soil profile becomes wetter and ultimately merges with the bottom layer.

107

108 The vegetation is classified into 12 plant functional types (Krinner et al., 2005) plus bare soil.
109 In these plant functional types, plants with a similar physiology are grouped together. The
110 SRC simulations in this paper further develop the “temperate deciduous broadleaf forest”
111 functional type.

112

113 As an extension to the standard version of ORCHIDEE, ORCHIDEE-FM was developed to
114 include a number of adaptations for forest management (Bellassen et al., 2010). These
115 adaptations include an age-related limitation of leaf area index (LAI) in young stands, an age-
116 related decline in NPP, self-thinning in unmanaged stands and anthropogenic thinning in
117 managed stands. The source code for this extended version can be found at
118 http://forge.ipsl.jussieu.fr/orchidee/browser/perso/toon.degroote/orchidee_FM.

119

120 **2.2 Model modifications to SRC**

121

122 **2.2.1 Management modifications**

123 A first and essential modification was the ability to simulate multiple rotations, incl. the
124 coppicing of the trees (Appendix A, teal sections). Under SRC, the trees are not entirely
125 harvested. A stump of approximately 10 cm is left, from which the trees can resprout
126 (DEFRA, 2004). To account for this, the biomass of 10-cm long stumps is calculated using
127 Eq. (1), and remains in the aboveground woody biomass pool, instead of contributing to the

128 exported biomass pool. Contrary to the thinning in ORCHIDEE-FM, only aboveground
129 biomass is removed during the coppicing of a short rotation coppice.

130
$$f_{bm_vol} \left(\sum \frac{L \cdot circ^2}{4\pi} \right) \quad \text{Eq. (1)}$$

131 where L is the length of the remaining stump (0.1 m), circ is the circumference of the
132 individual shoot, which is a variable in ORCHIDEE-FM and f_{bm_vol} is an allometric function
133 to calculate biomass from volume, as further described in section 2.2.2 and in Table 1.

134

135 A second modification was made for the cultivation regime at the site. In ORCHIDEE, trees
136 start their lives as saplings. Contrary to forest tree plantations, SRC plantations are established
137 using cuttings, i.e. 20-cm long hardwood sticks without any roots or leaves. The average
138 carbon content of a cutting was estimated from the average volume and wood density to be
139 2.5 g of C. ORCHIDEE was modified to grow SRC from these cuttings (Appendix A,
140 turquoise sections). Half of this C is located in the aboveground sapwood pool of the cutting
141 and the other half in the carbohydrate reserve. The number of cuttings per hectare can be
142 defined in the configuration file when running the model.

143

144 2.2.2 Growth modifications

145 Because ORCHIDEE is a big leaf model and does not simulate individual trees, ORCHIDEE-
146 FM uses allometric relations to convert and partition biomass. There are five allometric
147 relations to convert stem biomass into stem volume, stem volume into stem biomass,
148 circumference into stem volume, stem volume into circumference and circumference into
149 height (Table 1; Appendix A, blue sections). The functions f_{vol_bm} , f_{bm_vol} , f_{vol_circ} , and f_{circ_vol}
150 are used to partition the biomass into circumference categories and to calculate the biomass of
151 the initial hardwood cuttings from which the plantation is started. The function f_{height_circ}
152 calculates the height from the circumference. This height is used to calculate LAI and
153 roughness height. The roughness height is important in calculating the aerodynamic
154 resistance. These standard relations were parameterized using data from the Boom site, one of
155 the two SRC sites that we used for parameterization and evaluation (see 2.3.1).

156

157 After coppicing an SRC-tree resprouts as a multi-stemmed tree. This was incorporated into to
158 the model as a second growth modification (Appendix A, violet sections). The number of
159 shoots with which the tree resprouts depends on the genotype. The variation in the number of
160 stems resprouting after coppicing is very large, ranging from 1 to 25 (Pontailier et al.,
161 1999;Dillen et al., 2013). Here, we adopted an average across the many genotypes of two
162 stems after the first coppicing and four stems after the subsequent coppicing.

163

164 A final growth adaptation was made to the fine root growth. In ORCHIDEE, the senescence
165 of the leaves and fine roots occurs simultaneously by the same phenological trigger. For SRC
166 simulations, we decoupled the root mortality from the leaf senescence and included a turn-
167 over time (Appendix A, yellow sections). The poplar fine roots now stay alive for six months
168 after their formation, an average lifetime observed in the field (Coleman et al., 2000;Block et
169 al., 2006). The onset of fine root growth remains coupled with the phenological trigger for
170 leaf growth.

171

172 2.2.3 Allocation modifications

173 A poplar tree can become sexually mature from the age of five onwards, depending on the
174 genotype (Dickmann and Stuart, 1983;Muhle Larsen, 1963). Because the duration of most
175 SRC rotations is under five years, SRC-grown poplars will never produce flowers or seeds.
176 The same holds for the sapwood to heartwood conversion. To account for this in the model,
177 no carbon is allocated to the reproduction-pool (Appendix A, red sections), and no
178 aboveground sapwood is converted into heartwood (Appendix A, brown sections) when the
179 last coppicing was less than 5 years ago.

180

181 The tree species used in SRC plantations are fast-growing tree species that reach a large leaf
182 area as fast as they can. The standard allocation to leaves in ORCHIDEE-FM is strictly
183 constrained by the maximum leaf area index (LAI_{max}) for that year. This LAI_{max} evolves
184 slowly, as the stand grows and the canopy closes. The high planting density and the different
185 phenology of poplars in SRC plantations do not fit this scheme. Data show that for SRC
186 plantations, this limitation is only present in the first one to two years. Therefore, we adapted

187 LAI_{max} in the model such that it is only limited in the first year, and allowed to reach the plant
188 functional type-specific LAI_{max} from year 2 onwards (Appendix A, green sections).

189

190 After coppicing, poplar trees allocate almost no carbon to the growth of coarse roots. To
191 simulate this effect, the trees in the extended ORCHIDEE model try to maintain a prescribed,
192 structurally logical, root-shoot ratio. When the root-shoot ratio deviates from this prescribed
193 ratio by more than 10%, such as after removal of the entire shoot biomass, 95% of the C
194 allocated to wood production is allocated to the aboveground part (Appendix A, lime
195 sections).

196

197 2.2.4 Parameterization

198 The default parameters in ORCHIDEE were compared to measurements from the POPFULL
199 site (see Sect. 2.3.2). A number of parameters (Table 2) were changed based on this
200 comparison (Appendix A, pink sections). Parameters that were in the range of the measured
201 data were left unchanged. A first parameter is LAI_{max}. This is the maximal LAI that the trees
202 can reach. The next two parameters $V_{c,max}$ (maximum carboxylation rate) and J_{max} (maximum
203 electron transport rate) are photosynthetic parameters. When these parameters are higher,
204 photosynthesis will be higher. Next, H_{root} is the exponential decay factor of the root profile.
205 This parameter describes the distribution of the roots in the soil and therefore influences the
206 water availability to the plant. Finally, $\rho_{leaf,SW}$ and $\rho_{leaf,LW}$ are the short wave and long wave
207 leaf albedo. These parameters determine how much of the incoming radiation is absorbed by
208 the leaves and thus influence the energy uptake of the trees.

209

210 2.3 Data description

211 2.3.1 Boom site

212 The Boom site was poplar-based SRC plantation operating from April 1996 until November
213 2011 in Boom, near Antwerp, Belgium (51°05'N, 4°22'E; 5 m above sea level). The
214 plantation was established on a 0.56-ha former land fill, which was covered with a 2-m thick
215 soil layer. Seventeen different poplar (*Populus spp.*) genotypes, belonging to six parentage

216 lines, where planted in April 1996 in a double-row design with inter-row distances of 0.75 m
217 and 1.50 m and a spacing of 0.90 m within the rows, resulting in a planting density of 10 000
218 cuttings ha⁻¹. The plantation was harvested in December 1996, January 2001, February 2004,
219 February 2008 and November 2011, i.e. one establishment year and four subsequent rotations
220 of each 4 years, 3 years, 4 years and 4 years, respectively.

221 At this site dendrometric measurements included aboveground biomass, tree height and
222 circumference at 22 cm above ground level. A more complete description of the site and the
223 plant materials has been provided by Laureysens et al. (2003) and Casella and Ceulemans
224 (2002). The evolution of growth, biomass production and yield has been described in detail by
225 Dillen et al. (2011) and Dillen et al. (2013).

226

227 2.3.2 POPFULL site

228 The operationally managed POPFULL site was established in April 2010 in Lochristi, near
229 Ghent, Belgium (51°07'N, 3°51'E; 6 m above sea level), on 18.4 ha of former pasture and
230 cropland. Twelve different poplar (*Populus spp.*) genotypes and 3 willow (*Salix spp.*)
231 genotypes were planted in a double-row design with inter-row distances of 0.75 m and 1.50 m
232 and a spacing of 1.10 m within the rows, resulting in a planting density of 8000 cuttings ha⁻¹.
233 The plantation was harvested for the first time in February 2012.

234

235 At this site, an eddy covariance tower was erected (Zona et al., 2013a;2014;2013b). The
236 height of the tower varied between 3 m and 6 m, depending on canopy height. From this
237 tower, CO₂ and H₂O fluxes were measured. Furthermore, leaf phenology was monitored and
238 LAI was regularly measured. Soil temperature and soil moisture were also monitored during
239 2011. At the end of each growing season, the biomass production was estimated from stem
240 circumference measurements and site-specific allometric relations.

241 A complete description of this site is given in Broeckx et al. (2012), while the eddy
242 covariance flux measurements have been described in detail by Zona *et al.*
243 (2013b;2013a;2014) and the carbon budget was calculated by Verlinden et al. (2013b).

244

245 2.3.3 European biomass sites

246 For the evaluation of aboveground standing woody biomass production across Europe, we
247 used biomass measurements found in Njakou Djomo et al. (2015). From their list of sites, we
248 selected the 23 sites that were not irrigated and had poplar trees (Table 1).

249

250 Because meteorological data of sufficient resolution and a detailed site description for these
251 sites were not available, we could not perform a site-by-site comparison. Therefore, we
252 collected meteorological data from 22 different European sites in a similar geographical range
253 on the European Fluxes Database Cluster (<http://gaia.agraria.unitus.it/>, 1 September 2014) to
254 run our simulations. This way we could compare the range and trend of aboveground woody
255 biomass production along the latitudinal gradient, as well as along the annual precipitation
256 gradient and the average annual temperature gradient,

257

258 We selected sites with a public data access and open data use policy, for which data was
259 available for a minimum of five years (Table 1). Using this meteorological data, we ran the
260 model for 20 years, to calculate the mean annual aboveground standing woody biomass
261 production. For these simulations we chose a planting density of 10000 trees ha⁻¹ and a
262 rotation cycle of 2 years,

263 2.4 Simulation setup

264 Before running the actual simulations, a spinup was run to initialize the soil carbon pool for
265 every site. For this spinup the model was used without SRC modifications, with the standard
266 “temperate deciduous broadleaf forest” plant functional type. This spinup is performed by
267 running the model with the available input data repeatedly, until a soil carbon equilibrium is
268 reached. Because this takes a very long time, a part of this spinup is executed with simplified
269 versions of the model, i.e. teststomate and forcesoil. Teststomate deactivates sechiba, thus
270 only running the daily processes, instead of half-hourly processes, hereby accelerating the
271 model 48 times, reaching a steady state for the non-soil carbon pools. Forcesoil only uses the
272 ORCHIDEE's soil carbon module, reaching a steady state for the soil carbon pools.

273

274 For this spinup, the model was first run for 20 years, followed by 50 years with teststomate.
275 This was repeated three times. Thereafter, the model was run for 40 years, followed by 1000
276 years with forcesoil and finally another 260 years of the full model. This accumulates to a
277 total of 1510 years, of which 360 were run with the full model. The end state of the spinups is
278 then used as initial state for the actual simulations.

279

280 For the simulation of the POPFULL site, the soil fractions were set to the average of the
281 measured data (86% sand, 3% silt, 11% clay). For the Boom site, no texture data were
282 available. Being a former land fill, the soil description for this site was very imprecise,
283 mentioning only the broader texture classes, loam, sandy loam and silt loam. Therefore, the
284 standard texture values (49% sand, 29% silt, 22% clay), which correspond to loam, were used
285 for the Boom site. The number of cuttings was set to 8000 ha⁻¹ for the POPFULL site and
286 10 000 ha⁻¹ for the Boom site. The soil depth was set to 1 m for both sites.

287

288 **2.5 Data processing**

289 On the POPFULL site, meteo data for 2010 and 2011 were collected together with the eddy
290 covariance flux data. Since the measurements did not start until June 2010, this gap was filled
291 using data from a nearby station (Melle) from the Royal Meteorological Institute (RMI). For
292 the Boom site, meteo data were used from a nearby field site (Brasschaat).

293

294 For the POPFULL site, measured eddy covariance fluxes (GPP, R_{eco}, NEE, H and LE) were
295 used to evaluate the model outputs. These data were not related to the data that were used to
296 calibrate the model. NEE, H and LE were measured directly by the eddy covariance
297 technique, but for GPP and R_{eco} an approximation had to be calculated using flux-partitioning.
298 Here, GPP and R_{eco} were calculated using the online eddy-covariance gap-filling and flux-
299 partitioning tool of the Max Planck Institute for Biogeochemistry ([http://www.bgc-
300 jena.mpg.de/~MDIwork/eddyproc/](http://www.bgc-jena.mpg.de/~MDIwork/eddyproc/)), which is based on the standardized methods described in
301 Reichstein et al. (2005).

302

303 To quantify the model fit of the modelled fluxes with the measured data, three statistical
304 criteria for model efficiency were evaluated using the half hourly data. The coefficient of
305 determination (R^2), the normalised root mean square error (NRMSE) and a Pearson
306 correlation coefficient (PCC) were calculated. The root mean square error was normalised by
307 dividing it by the range of values of the measured variable.

308 R^2 explains the variance in model performance by comparing it to the data variation. The
309 NRMSE gives a measure for the accumulated model error. The PCC shows how well the data
310 is correlated. While R^2 and PCC give a measure for how well the trends in the data are
311 simulated, NRMSE gives a measure for the total cumulated model error

312 To visualise the model fit, the modelled fluxes were plotted against the measured weekly
313 averages.

314

315 To compare the total fluxes, the half hourly data were cumulated. Since there were no flux
316 measurements before June 2010, this gap was filled with the modelled data.

317

318 **3 Results & Discussion**

319 The relative impact of the model modifications on the accuracy of the model simulations by
320 the extended model, ORCHIDEE-SRC, relative to ORCHIDEE-FM is presented in Fig. 1.
321 Biomass production and all fluxes were simulated better or equally well by the extended
322 model. Fig. 2 also shows the improvement in the simulation of biomass production compared
323 to ORCHIDEE-FM. Detailed analysis of the model simulations of biomass production,
324 carbon fluxes, energy fluxes and soil parameters are given in the sections below.

325

326 **3.1 Biomass evaluation**

327 **3.1.1 Site level**

328 For the Boom site, the yearly aboveground biomass measurements were compared to the
329 model output (Fig. 2a). From the third year of the first rotation onwards, the model
330 predictions were well within the range of measured values and approximate the average
331 aboveground woody biomass production. Measurements were available for 17 genotypes,

332 hence the wide range in observations. The low measured values in the first two years might be
333 explained by strong competition from weeds, which was observed in the starting years of this
334 plantation (R. Ceulemans, personal communication). The low values for the year 1998 – a
335 cold wet year – are explained by a severe rust infection at the site (Al Afas et al., 2008).

336

337 The modelled aboveground biomass for the POPFULL site was also well within the measured
338 ranges (Fig. 2b), although the prediction for the first year was in the lower limits of the range.

339

340 3.1.2 Europe

341 Since we couldn't simulate the same sites as we collected measurements for, we compared the
342 average annual aboveground standing woody biomass for the sites across Europe based on
343 their latitude, average annual temperature and average annual precipitation (Fig. 3).

344

345 The simulations were within the range of the measured values and followed their general
346 trends. When comparing with latitude, increasing latitudes increase biomass production up to
347 around 55°N. The biomass production of simulations for latitudes above 55°N start declining
348 again, but can't be compared to measurements, because of lacking data (Fig. 3a). Increasing
349 temperatures have a negative effect on aboveground woody biomass production for both the
350 measurements and the simulations (Fig. 3b). This is probably caused by the negative relation
351 between temperature and precipitation. The simulated aboveground biomass production
352 increases slightly with increasing precipitation (Fig 3c). This trend is also shown by the
353 measured data, except for two high producing sites in the low precipitation range.

354

355 Generally, the measured data had a higher spread, which could be explained by variable
356 factors we could not account for in the general modelling approach. Such factors could
357 include genotype selection, weed competition, rotation length, planting density, etc.

358 3.2 CO₂ flux evaluation

359 The measured C and energy fluxes at the POPFULL site were compared to the model outputs.
360 Fig. 4 depicts both the simulated and observed cumulative GPP, NEE, H, LE and R_{eeco}.

361

362 During the first year, the calculated and observed GPP values matched well ($R^2 = 0.78$,
363 NRMSE = 0.064, PCC = 0.89; Fig. 4). In winter, measured values established a slight
364 increasing trend, while GPP remained constant in the model outputs. This could either be
365 explained by photosynthesis of weeds, which are not represented in the model, or by errors in
366 the flux partitioning. During the second year, the modelled GPP started rising about one
367 month later than the measured values, but thereafter caught up with the measurements
368 (Fig. 4). Again, this difference might have been caused by the presence of weeds in the field,
369 which were not accounted for in the model. Another reason for these differences could be the
370 use of different genotypes at the field site, while the model only simulates an average
371 genotype. In 2011, the spring bud flushing date of the different genotypes ranged from day 72
372 until day 107, which is about a one month difference. The modelled bud flush started on day
373 97, which is well within this observed range, but logically results in a lag of 25 days between
374 observed and simulated date of onset of GPP. After two years, the cumulated GPP values
375 were 23.0 Mg C ha⁻¹ and 21.4 Mg C ha⁻¹ for the model and the measurements, respectively.
376 This difference of 1.6 Mg C ha⁻¹, represents an overestimation by the model of only 7%, well
377 within the uncertainty of eddy covariance-based GPP estimates (Desai et al., 2008; Richardson
378 et al., 2006).

379

380 The modelled R_{eco} fitted the measurements very well ($R^2 = 0.95$, NRMSE = 0.078 PCC =
381 0.91). The only point of divergence was the dry spell in the summer of the second year. Here,
382 R_{eco} was underestimated, probably because the model is too sensitive to drought. The
383 accumulated R_{eco} for the first rotation based on observations was 24.0 Mg C ha⁻¹, while the
384 model predicted 23.3 Mg C ha⁻¹; an underestimation of only 3%.

385

386 C is taken up by photosynthesis (GPP) and emitted through respiration (R_{eco}). The resulting
387 net flux is NEE. Small errors in GPP and R_{eco} might therefore accumulate in NEE giving it a
388 worse fit. When comparing NEE, the fit is less good than for GPP and R_{eco} ($R^2 = 0.51$,
389 NRMSE = 0.069, PCC = 0.84). In the model results, the plantation switched from emitting C
390 to taking up C in July of the first year. In the measured data, this switch occurred only during
391 August, possibly because of the increased C loss due to the land use change after the
392 plantation establishment (Zona et al., 2013a). During the winter and spring of the second

393 growing season, both the simulated and the measured fluxes indicated a net loss of CO₂, but
394 the simulation suggested a stronger source. This difference could probably be explained by
395 the presence of weeds on the site, which were not present in the model simulation. The
396 photosynthesis of these weeds partly counteracted the C losses from soil respiration. From
397 August until October, both the model and the measurements indicated a C uptake. The model,
398 however, presented a stronger C sink than the measurements. From October onwards, both
399 modelled and measured data showed a C source. At the end of the second year, the end of the
400 first rotation, the measurements showed a cumulated net C loss of 5.4 Mg ha⁻¹, while the
401 model only predicted a C loss of 3.3 Mg ha⁻¹. The model underestimated the C loss to the
402 atmosphere by 39%.

403

404 A good fit for GPP and R_{eco} is, however, more important than an accurate simulation of NEE,
405 because they are the real (and large) physical fluxes that occur in the field, and are simulated
406 by the model. Also the soil C loss was simulated adequately. The measured soil C loss was
407 700 g m⁻² for the top 15 cm (Verlinden et al., 2013a), while the model predicted a soil C loss
408 of 740 g m⁻² over the first rotation.

409

410 **3.3 Water and energy flux evaluation**

411 For H, the cumulative plot (Fig. 4) shows diverging lines and an overestimation of 120% of
412 the cumulative energy loss from H at the end of the rotation ($R^2 = 0.36$, NRMSE = 0.057,
413 PCC = 0.71). The error is probably caused by a stable stratification that often develops in
414 dense plantations at night. Because of this stratification the measured sensible heat flux at
415 night is lower than the simulated flux. The averaged diurnal pattern shown in the insert of Fig.
416 4 clearly shows this discrepancy. The stratification cannot be represented correctly by the
417 calculation of surface drag, in the way it is implemented in ORCHIDEE. This problem did
418 already exist in the model, as described by Krinner et al. (2005). Because H has no impact on
419 the C or water cycle in the model algorithms, this problem was not considered an issue in this
420 study.

421

422 During the first growing season, LE increased slower in the model than can be observed in the
423 measured data ($R^2 = 0.68$, NRMSE = 0.055, PCC = 0.78; Fig. 4). This might be explained by
424 the LAI. The modelled LAI (LAI_{max} 0.75) for the first year was on the lower end of the
425 measured LAI ranges (LAI_{max} 0.6 – 1.8). This lower leaf area consequently resulted in a lower
426 leaf surface to evaporate water from. From November of the first year onward, the cumulative
427 LE curves of the simulations and the measurements keep running in parallel, except for a
428 small period during the second year. This was caused by a dry spell during August. The
429 model slightly underestimated the effect of the drought, allowing the trees to transpire more
430 water. This can be observed in Fig. 5, as the six highlighted dots that represent the six dry
431 weeks that are marked in Fig. 6b. At the end of the rotation, this resulted in a cumulative LE
432 of 880 kW m^{-2} for the measurements and 806 kW m^{-2} for the model, which is an
433 underestimation of 8% by the model.

434

435 **3.4 Soil variables evaluation**

436 Fig. 6a shows the measured and modeled soil temperature during 2011 for the POPFULL site.
437 This is the only data we had available on soil temperature. This data shows that the soil
438 temperature was simulated very well by our model ($R^2 = 0.955$, NRMSE = 0.098, PCC =
439 0.907).

440

441 For soil moisture, ORCHIDEE only has two soil compartments, of which one is only present
442 after rainfall (Fig. 6b). We compared the total simulated soil water content to the average
443 measured soil water content of the top 50 cm of soil, which had a reasonable fit ($R^2 = 0.976$,
444 NRMSE = 0.152, PCC = 0.828). Due to the simplicity of the implementation of soil moisture
445 in ORCHIDEE, the model cannot simulate the level of detail that is shown by the
446 measurements. The model does, however, very clearly show the decline of soil water content
447 during the dry spell, and the replenishment of the top layer with the precipitation after the dry
448 spell.

449

450 **4 Conclusion**

451 Our validation shows that the modifications to the model ORCHIDEE presented in this paper
452 perform well to predict aboveground harvestable woody biomass. Also gross primary
453 production ($R^2 = 0.78$, NRMSE = 0.064, PCC = 0.89) and ecosystem respiration ($R^2 = 0.95$,
454 NRMSE = 0.078 PCC = 0.91) were simulated very well. Also soil temperature and soil
455 moisture are simulated adequately, but due to the simplicity of the soil moisture simulation,
456 there are some discrepancies, which also influence the simulation of the latent heat flux. The
457 annual latent heat flux was, however, simulated reasonably well. Overall the ORCHIDEE-
458 SRC version of the ORCHIDEE model is very well suited to simulate biomass production in
459 SRC plantations.

460

461 **5 Acknowledgements**

462 The research leading to these results has received funding from the European Research
463 Council under the European Commission's Seventh Framework Programme (FP7/2007-2013)
464 as ERC grant agreement n°. 233366 (POPFULL), the Flemish Hercules Foundation as
465 Infrastructure contract ZW09-06, the Flemish Methusalem Programme, the Research Council
466 of the University of Antwerp, and the Research Foundation – Flanders (FWO; DOFOCO
467 project). We gratefully acknowledge the excellent technical support of Joris Cools and the
468 logistic support of Kristof Mouton at the field site. T. De Groote is a Ph. D. fellow of the
469 Research Foundation – Flanders (FWO) and the Flemish Institute for Technological Research
470 (VITO)

471

472 **6 References**

473 Al Afas, N., Marron, N., Van Dongen, S., Laureysens, I., and Ceulemans, R.: Dynamics of
474 biomass production in a poplar coppice culture over three rotations (11 years), *Forest*
475 *Ecology and Management*, 255, 1883-1891, 10.1016/j.foreco.2007.12.010, 2008.

476 Aylott, M. J., Casella, E., Tubby, I., Street, N. R., Smith, P., and Taylor, G.: Yield and
477 spatial supply of bioenergy poplar and willow short-rotation coppice in the UK, *New*
478 *Phytologist*, 178, 358-370, 2008.

479 Bellassen, V., Le Maire, G., Dhote, J. F., Ciais, P., and Viovy, N.: Modelling forest
480 management within a global vegetation model Part 1: Model structure and general
481 behaviour, *Ecological Modelling*, 221, 2458-2474, 2010.

482 Block, R. M. A., Rees, K. C. J., and Knight, J. D.: A review of fine root dynamics in
483 *Populus* plantations, *Agroforest Syst*, 67, 73-84, DOI 10.1007/s10457-005-2002-7,
484 2006.

485 Broeckx, L. S., Verlinden, M. S., and Ceulemans, R.: Establishment and two-year growth
486 of a bio-energy plantation with fast-growing *Populus* trees in Flanders (Belgium): Effects
487 of genotype and former land use, *Biomass & Bioenergy*, 42, 151-163, 2012.

488 Casella, E., and Ceulemans, R.: Spatial distribution of leaf morphological and
489 physiological characteristics in relation to local radiation regime within the canopies of 3-
490 year-old *Populus* clones in coppice culture, *Tree Physiology*, 22, 1277-1288, 2002.

491 Choisnel, E.: Le bilan d'énergie et le bilan hydrique du sol, *La Météorologie*, 6, 103-133,
492 1977.

493 Coleman, M. D., Dickson, R. E., and Isebrands, J. G.: Contrasting fine-root production,
494 survival and soil CO₂ efflux in pine and poplar plantations, *Plant Soil*, 225, 129-139, Doi
495 10.1023/A:1026564228951, 2000.

496 DEFRA: Growing short rotation coppice - Best practice guidelines for applicants to Defra's
497 energy crops scheme, Department for Environment, Food and Rural Affairs, London, UK,
498 2004.

499 Desai, A. R., Richardson, A. D., Moffat, A. M., Kattge, J., Hollinger, D. Y., Barr, A., Falge,
500 E., Noormets, A., Papale, D., Reichstein, M., and Stauch, V. J.: Cross-site evaluation of
501 eddy covariance GPP and RE decomposition techniques, *Agr Forest Meteorol*, 148, 821-
502 838, DOI 10.1016/j.agrformet.2007.11.012, 2008.

503 Dickmann, D., and Stuart, K. W.: The culture of poplars in eastern North America, Dept.
504 of Forestry, Michigan State University, East Lansing, Mich. and Dansville, 1983.

505 Dillen, S. Y., Vanbeveren, S., al Afas, N., Laureysens, I., Croes, S., and Ceulemans, R.:
506 Biomass production in a 15-year-old poplar short-rotation coppice culture in Belgium,
507 *Aspects of applied biology*, 112, 99-106, 2011.

508 Dillen, S. Y., Djomo, S. N., Al Afas, N., Vanbeveren, S., and Ceulemans, R.: Biomass
509 yield and energy balance of a short-rotation poplar coppice with multiple clones on
510 degraded land during 16 years, *Biomass & Bioenergy*, 56, 157-165, 2013.

511 Ducoudre, N. I., Laval, K., and Perrier, A.: Sechiba, a New Set of Parameterizations of
512 the Hydrologic Exchanges at the Land Atmosphere Interface within the Lmd Atmospheric
513 General-Circulation Model, *Journal of Climate*, 6, 248-273, 1993.

514 EC: Communication from the commision - Europe 2020 - A strategy for smart,
515 sustainable and inclusive growth. COM 2010;2020. Final (03/03/2010), European
516 Commission, Brussels, 2010.

517 Hansen, E. A.: Poplar Woody Biomass Yields - a Look to the Future, *Biomass &*
518 *Bioenergy*, 1, 1-7, 1991.

519 Herve, C., and Ceulemans, R.: Short-rotation coppiced vs non-coppiced poplar: A
520 comparative study at two different field sites, *Biomass & Bioenergy*, 11, 139-150, Doi
521 10.1016/0961-9534(96)00028-1, 1996.

522 Krinner, G., Viovy, N., de Noblet-Ducoudre, N., Ogee, J., Polcher, J., Friedlingstein, P.,
523 Ciais, P., Sitch, S., and Prentice, I. C.: A dynamic global vegetation model for studies of
524 the coupled atmosphere-biosphere system, *Global Biogeochemical Cycles*, 19, GB1015,
525 2005.

526 Laureysens, I., Deraedt, W., Indeherberge, T., and Ceulemans, R.: Population dynamics
527 in a 6-year old coppice culture of poplar. I. Clonal differences in stool mortality, shoot
528 dynamics and shoot diameter distribution in relation to biomass production, *Biomass &*
529 *Bioenergy*, 24, 81-95, 2003.

530 Muhle Larsen, C.: Considérations sur l'amélioration du genre *Populus* et spécialement sur
531 la section *Aigeiros* 63-2b/9, 1963.

532 Njakou Djomo, S., Ac, A., Zenone, T., De Groote, T., Bergante, S., Facciotto, G., Sixto,
533 H., Ciria Ciria, P., Weger, J., and Ceulemans, R.: Energy performances of intensive and
534 extensive short rotation cropping systems for woody biomass production in the EU,
535 *Renewable and Sustainable Energy Reviews*, 41, 845-854,
536 <http://dx.doi.org/10.1016/j.rser.2014.08.058>, 2015.

537 Pontailier, J. Y., Ceulemans, R., and Guittet, J.: Biomass yield of poplar after five 2-year
538 coppice rotations, *Forestry*, 72, 157-163, 1999.

539 Reichstein, M., Falge, E., Baldocchi, D., Papale, D., Aubinet, M., Berbigier, P., Bernhofer,
540 C., Buchmann, N., Gilmanov, T., Granier, A., Grunwald, T., Havrankova, K., Ilvesniemi,
541 H., Janous, D., Knohl, A., Laurila, T., Lohila, A., Loustau, D., Matteucci, G., Meyers, T.,
542 Miglietta, F., Ourcival, J. M., Pumpanen, J., Rambal, S., Rotenberg, E., Sanz, M.,
543 Tenhunen, J., Seufert, G., Vaccari, F., Vesala, T., Yakir, D., and Valentini, R.: On the
544 separation of net ecosystem exchange into assimilation and ecosystem respiration:
545 review and improved algorithm, *Global Change Biology*, 11, 1424-1439, 2005.

546 Richardson, A. D., Hollinger, D. Y., Burba, G. G., Davis, K. J., Flanagan, L. B., Katul, G.
547 G., Munger, J. W., Ricciuto, D. M., Stoy, P. C., Suyker, A. E., Verma, S. B., and Wofsy, S.
548 C.: A multi-site analysis of random error in tower-based measurements of carbon and
549 energy fluxes, *Agr Forest Meteorol*, 136, 1-18, DOI 10.1016/j.agrformet.2006.01.007,
550 2006.

551 Verlinden, M. S., Broeckx, L. S., Wei, H., and Ceulemans, R.: Soil CO₂ efflux in a
552 bioenergy plantation with fast-growing *Populus* trees - influence of former land use,
553 inter-row spacing and genotype, *Plant Soil*, 369, 631-644, DOI 10.1007/s11104-013-
554 1604-5, 2013a.

555 Verlinden, M. S., Broeckx, L. S., Zona, D., Berhongaray, G., De Groote, T., Camino
556 Serrano, M., Janssens, I. A., and Ceulemans, R.: Net ecosystem production and carbon

557 balance of an SRC poplar plantation during its first rotation, *Biomass and Bioenergy*, 56,
558 412-422, 10.1016/j.biombioe.2013.05.033, 2013b.

559 Zervos, A., Lins, C., and Tesnière, L.: EU Roadmap - Mapping Renewable Energy
560 Pathways towards 2020, European Renewable Energy Council, Brussels, Belgium, 104,
561 2011.

562 Zona, D., Janssens, I. A., Aubinet, M., Gioli, B., Vicca, S., Fichot, R., and Ceulemans, R.:
563 Fluxes of the greenhouse gases (CO₂, CH₄ and N₂O) above a short-rotation poplar
564 plantation after conversion from agricultural land, *Agr Forest Meteorol*, 169, 100-110,
565 DOI 10.1016/j.agrformet.2012.10.008, 2013a.

566 Zona, D., Janssens, I. A., Gioli, B., Jungkunst, H. F., Serrano, M. C., and Ceulemans, R.:
567 N₂O fluxes of a bio-energy poplar plantation during a two years rotation period, *GCB*
568 *Bioenergy*, 5, 536-547, 10.1111/gcbb.12019, 2013b.

569 Zona, D., Gioli, B., Fares, S., De Groote, T., Pilegaard, K., Ibrom, A., and Ceulemans, R.:
570 Environmental controls on ozone fluxes in a poplar plantation in Western Europe,
571 *Environmental Pollution*, 184, 201-210, 2014.

572

573

574 **7 Tables and Figures**

575 **7.1 Tables**

576 Table 1: Allometric relations used for the SRC simulation in the ORCHIDEE-FM
 577 model and their parameter values. SRC = short rotation coppice culture.

Formula	Parameter	Value	Unit
$f_{vol_bm} \rightarrow volume = \frac{biomass}{density}$	density	1.25e5	g C m ⁻³
$f_{bm_vol} \rightarrow biomass = volume \cdot density$			
$f_{vol_circ} \rightarrow volume = \sum \frac{a \cdot \left(\frac{circumference}{\pi} \right)^b}{density}$	density	1.25e5	g C m ⁻³
	a	0.033	
	b	2.6	
$f_{circ_vol} \rightarrow circumference = \pi \cdot \left(\frac{volume \cdot density}{a} \right)^{1/b}$			
	a	17.2684	
$f_{height_circ} \rightarrow height = a \cdot circumference^b$	b	0.6791	

578

579 Table 2: Parameter values that were changed between the standard version of
 580 ORCHIDEE-FM and the adapted version for SRC simulation. LAI_{max} = maximal leaf
 581 area index, V_{c,max} = maximum rate of carboxylation, J_{max} = maximum electron
 582 transport rate, H_{root} = exponential decay factor of the root profile, ρ_{leaf,SW} = short wave
 583 leaf albedo, ρ_{leaf,LW} = long wave leaf albedo.

Parameter	Unit	ORCHIDEE PFT 6	ORCHIDEE-SRC
LAI _{max}	m ² m ⁻²	4.5	2.5
V _{c,max}	μmol m ⁻² s ⁻¹	55	130
J _{max}	μmol m ⁻² s ⁻¹	70	180
H _{root}		0.8	1.5
ρ _{leaf,SW}		0.06	0.20
ρ _{leaf,LW}		0.22	0.30

Table 3: Biomass validation site info for the simulated sites, acquired from the European Fluxes Database Cluster (<http://gaia.agraria.unitus.it/>, 1 September 2014) and the measured sites, acquired from (Njakou Djomo et al., 2015).

Simulations						Measurements					
Country	Site name	Latitude	Longitude	Annual temp °C	Annual precip mm	Country	Site name	Latitude	Longitude	Annual temp °C	Annual precip mm
PT	Mitra IV (Tojal)	38.48 N	8.02 W	14.2	588	IT	Caramagna piemonte	44.47 N	7.44 E	12.5	700
ES	Las Majadas del Tietar	39.94 N	5.77 W	16.1	721	IT	Lombriasco	44.51 N	7.38 E	13.0	650
IT	Collelongo	41.85 N	13.59 E	7.3	1160	CZ	Nová Olešná	49.17 N	15.16 E	7.2	730
IT	Roccarespampani 1	42.41 N	11.93 E	15.6	840	CZ	Bystřice	49.21 N	12.48 E	5.7	800
FR	Mauzac	43.39 N	1.29 E	12.7	566	CZ	Smilkov	49.36 N	14.36 E	6.8	650
IT	San Rossore	43.73 N	10.28 E	15.2	921	CZ	Rosice	50.03 N	15.42 E	8.5	500
FR	Puechabon	43.74 N	3.6 E	13.6	894	DE	Arnsfeld	50.34 N	13.06 E	7.0	625
IT	Lavarone	45.96 N	11.28 E	6.9	1263	DE	Großschirma	50.57 N	13.17 E	7.2	820
IT	Renon	46.59 N	11.43 E	4.5	1219	DE	Krummenhennersdorf	50.98 N	13.36 E	7.2	820
AT	Neustift	47.12 N	11.32 E	6.8	700	BE	Zwijnaarde	51.02 N	3.43 E	9.8	821
CZ	Laegern	47.48 N	8.37 E	7.7	777	BE	Boom	51.05 N	4.22 E	11.1	824
DE	Wetzstein	50.45 N	11.46 E	6.5	971	BE	Lochristi	51.06 N	3.51 E	9.5	726
DE	Klingenberg	50.89 N	13.52 E	7.6	801	DE	Commichau	51.08 N	12.50 E	8.5	680
DE	Grillenburg	50.95 N	13.51 E	8.5	975	DE	Skäßchen	51.20 N	13.35 E	8.5	575
DE	Tharandt	50.96 N	13.57 E	8.6	871	DE	Großthiemig	51.22 N	13.4 E	8.5	575
DE	Hainich	51.08 N	10.45 E	8.3	779	DE	Thammenhain	51.25 N	12.51 E	8.5	575
BE	Brasschaat	51.31 N	4.52 E	10.6	848	DE	Nochten	51.25 N	14.36 E	8.5	650
UK	Pang/Lambourne forest	51.45 N	1.27 W	12.3	658	DE	Vetschau	51.46 N	14.04 E	8.5	550
NL	Loobos	52.17 N	5.74 E	10.0	872	DE	Methau I	51.50 N	12.51 E	8.1	690
DK	Soroe	55.49 N	11.64 E	8.4	760	DE	Methau II	51.50 N	12.51 E	8.1	690
RU	Fyodorovskoye	56.46 N	32.92 E	5.1	524	DE	Kuhstorf	53.23 N	11.15 E	8.2	616
FI	Hyytiälä	61.85 N	24.3 E	4.1	555	DE	Laage	53.55 N	12.20 E	8.0	630

586 **7.2 Figures**

587 Fig. 1: Comparison between the performance of the ORCHIDEE-SRC and
588 ORCHIDEE-FM. The relative error was calculated as the relative difference between
589 the field measurements and the model simulations. The green background indicates an
590 improvement by the extended model relative to ORCHIDEE-FM, the red background
591 indicates a deterioration of the model results from the extended model. A darker
592 colour indicates a more pronounced difference. The Boom site simulations are shown
593 as filled circles and the POPFULL site simulations are shown as open circles. The
594 letters next to the symbol are: GPP = gross primary productivity cumulated over the
595 two measurement years; Reco = ecosystem respiration cumulated over the two
596 measurement years; NEE = net ecosystem exchange cumulated over the two
597 measurement years; LE = latent heat cumulated over the two measurement years; H =
598 sensible heat cumulated over the two measurement years; Bx = aboveground woody
599 biomass production of rotation x.

600

601 Fig. 2: The simulated standing aboveground woody biomass (a) for the Boom site and
602 (b) for the POPFULL site. The solid black line is the biomass simulated by the
603 extended model, ORCHIDEE-SRC. The dashed line is the biomass simulated by the
604 standard version of ORCHIDEE-FM, with only coppicing implemented. The symbols
605 are the different parentages of the poplars at that site and the gray area is the range of
606 measured biomasses. The parentages are *Populus trichocarpa* × *P. balsamifera*
607 (T×B), *P. trichocarpa* × *P. deltoides* (T×D), *P. trichocarpa* (T), *P. deltoides* × *P.*
608 *nigra* (D×N), *P. deltoides* × *P. trichocarpa* (D×T), *P. nigra* (N), *P. canadensis* (C), *P.*
609 *deltoides* × (*P. trichocarpa* × *P. deltoides*) (D×(T×D)), *P. trichocarpa* × *P.*
610 *maximowiczii* (T×M).

611

612 Fig. 3: Comparison of aboveground standing woody biomass for ORCHIDEE-SRC
613 simulations (open diamonds) across Europe with site measurements (black circles)
614 across Europe. The biomass is plotted against (A) latitude, (B) annual average
615 temperature and (C) annual precipitation.

616

617 Fig. 4: Cumulative fluxes of gross primary production (GPP), ecosystem respiration
618 (R_{eco}), net ecosystem exchange (NEE), sensible heat (H) and latent heat (LE) for the
619 POPFULL site. The insert in the graph for sensible heat flux shows the average
620 diurnal cycle of the sensible heat flux. The thin solid lines are the measured values
621 from the eddy-covariance measurements or recalculated from these measurements
622 using the flux-partitioning tool of the Max Planck Institute for Biogeochemistry
623 (<http://www.bgc-jena.mpg.de/~MDIwork/eddyproc/>). The dashed line are the model
624 outputs using the standard model ORCHIDEE-FM. The solid thick lines are the model
625 outputs using the modified model ORCHIDEE-SRC. Since there were no flux
626 measurements before June 2010, both simulated and measured values coincide before
627 that date.

628

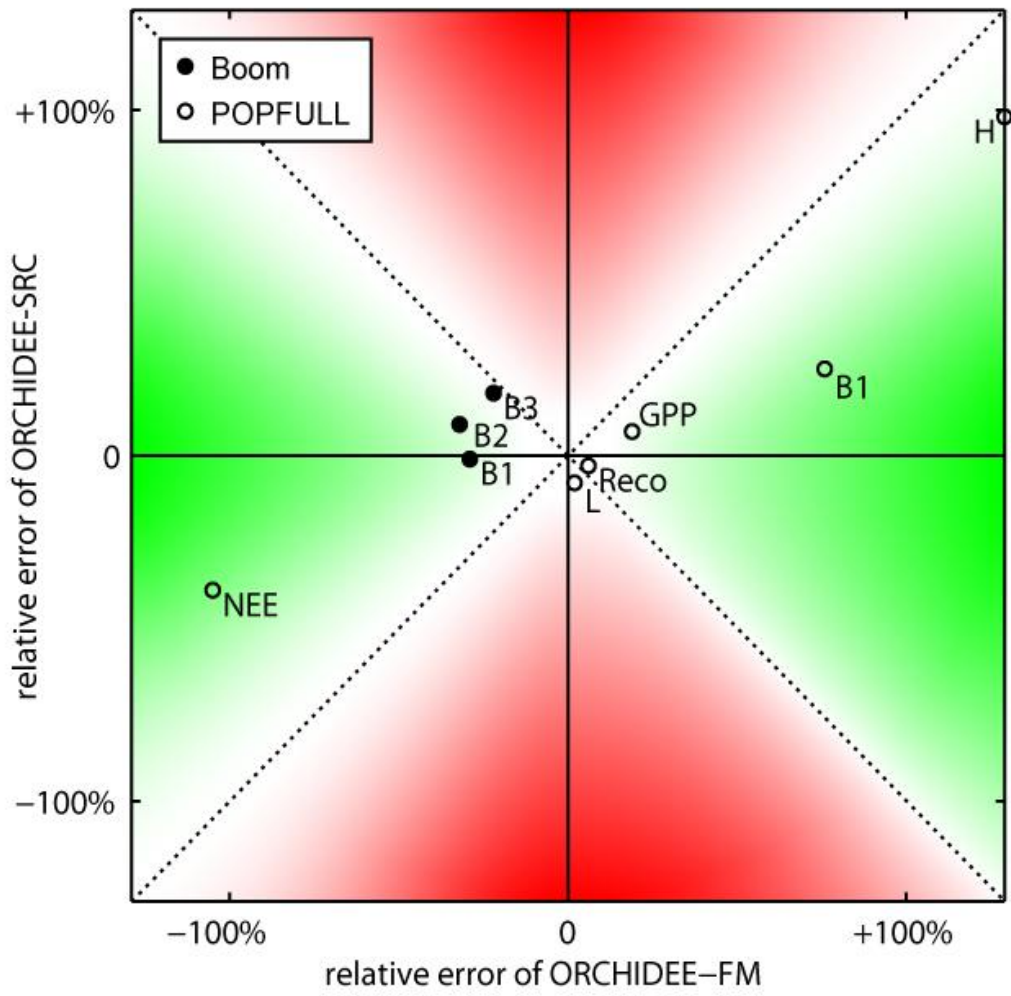
629 Fig. 5: A 1-to-1 comparison of weekly averages of latent heat (LE) for the POPFULL
630 site, between the model outputs and the measured values. The dotted line is the 1:1
631 line. Weeks 18-23 which represent the dry spell are highlighted as grey circles.

632

633 Fig. 6: A comparison of modelled and measured soil state variables for 2011 at the
634 POPFULL site. (A) shows the daily average soil temperature simulated (fat) and
635 measured (thin). (B) shows the soil water content. The gray area represents the
636 measured range of soil water content values for the top 50 cm of the soil. The dotted
637 line is the soil water content of the lower soil water compartment of the model and the
638 solid line is the total soil water content of the upper and lower soil water
639 compartments.

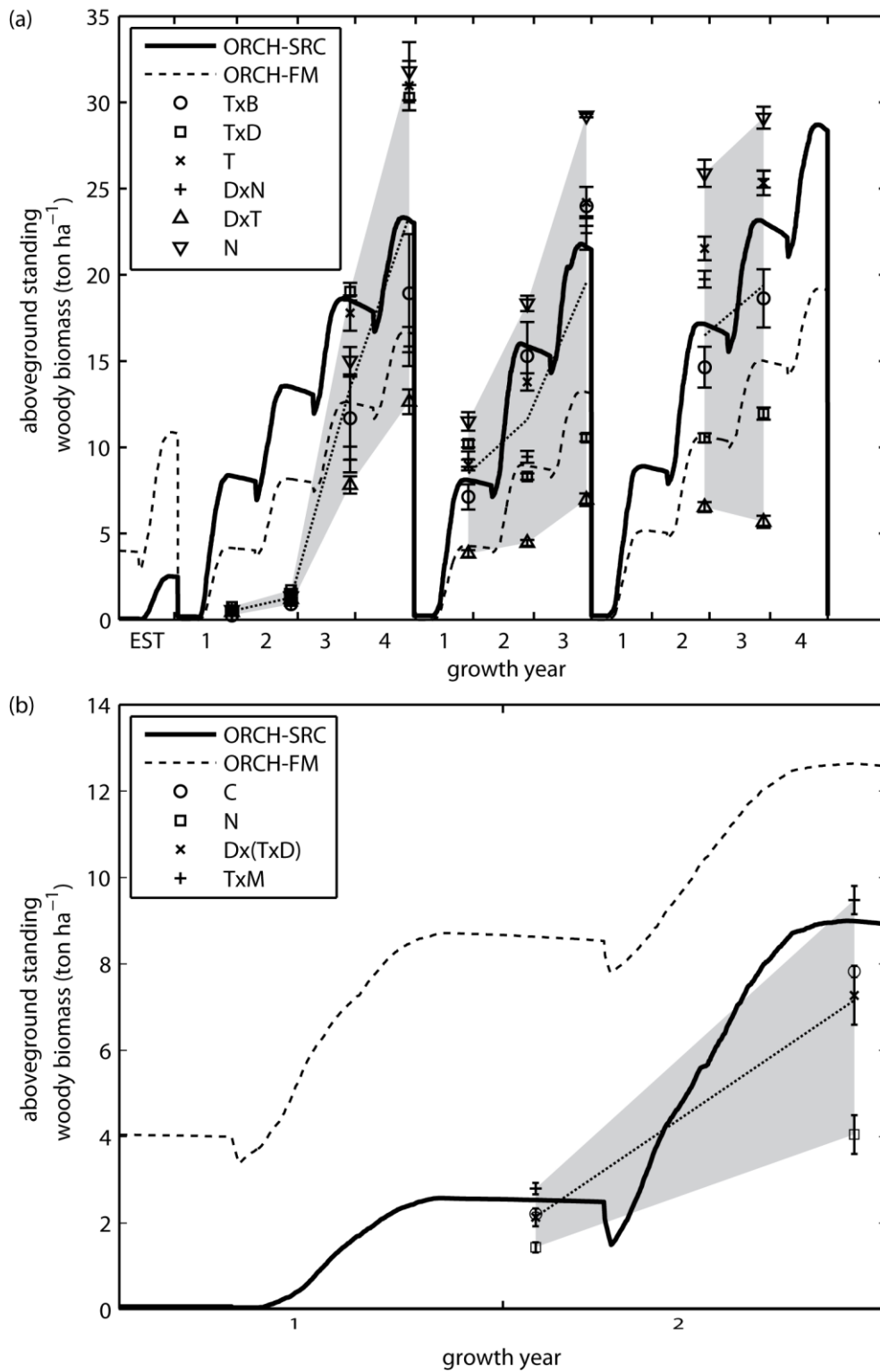
640

641 Fig. 1



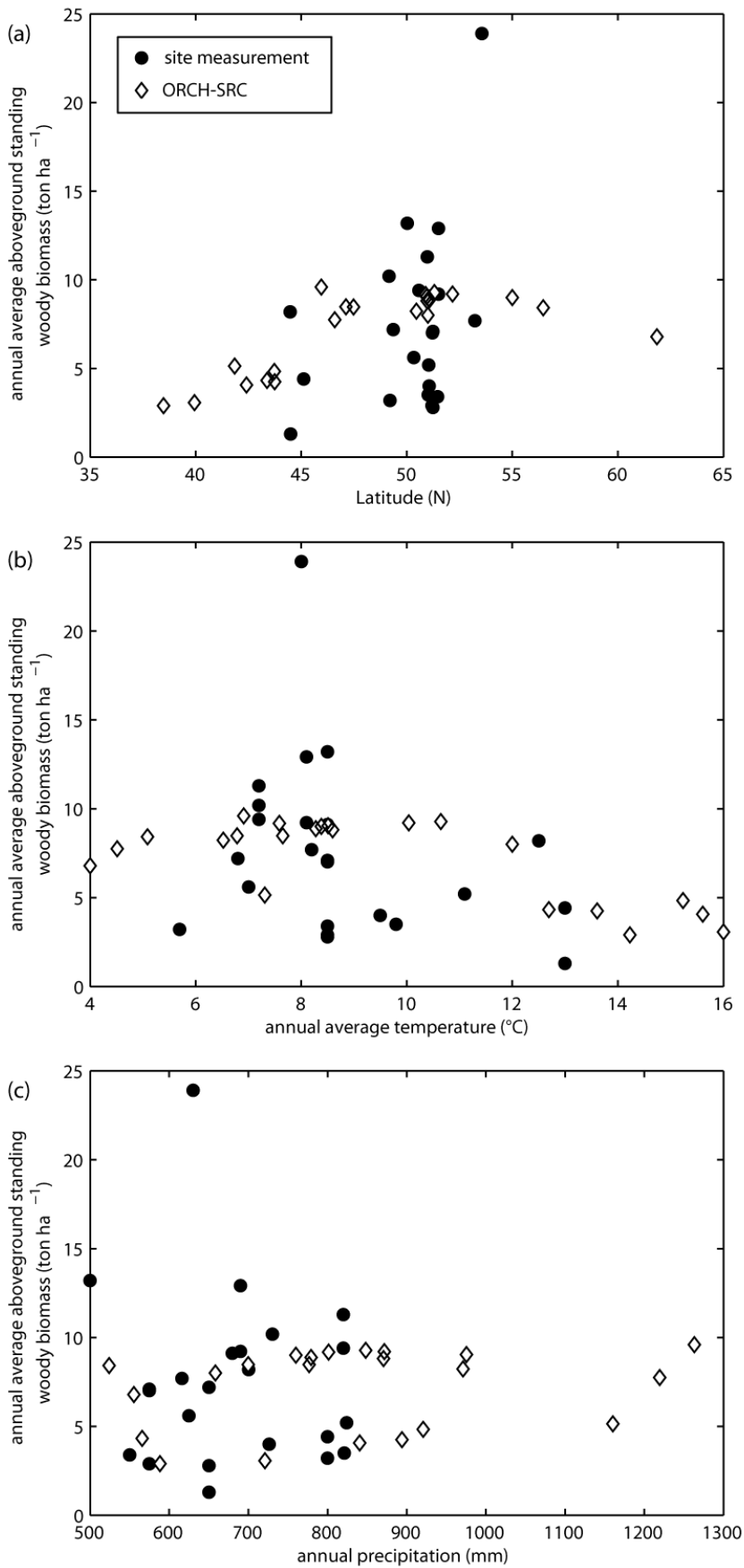
642
643

644 Fig. 2



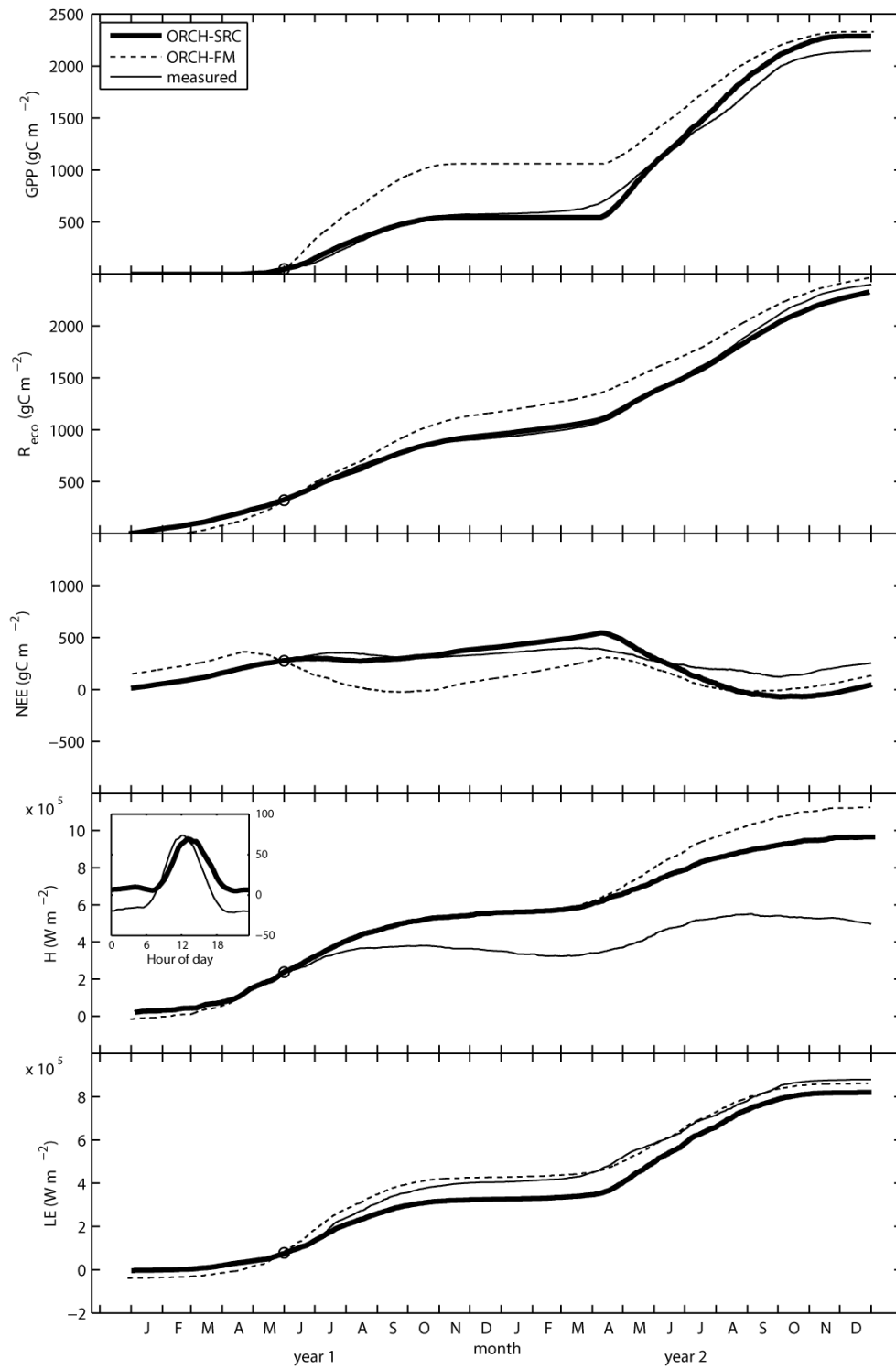
645
646

647 Fig. 3



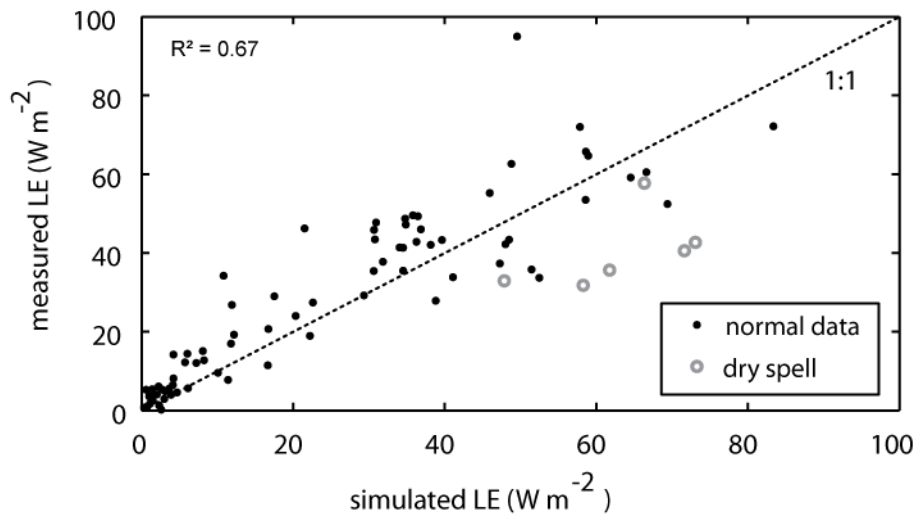
648

649 Fig. 4



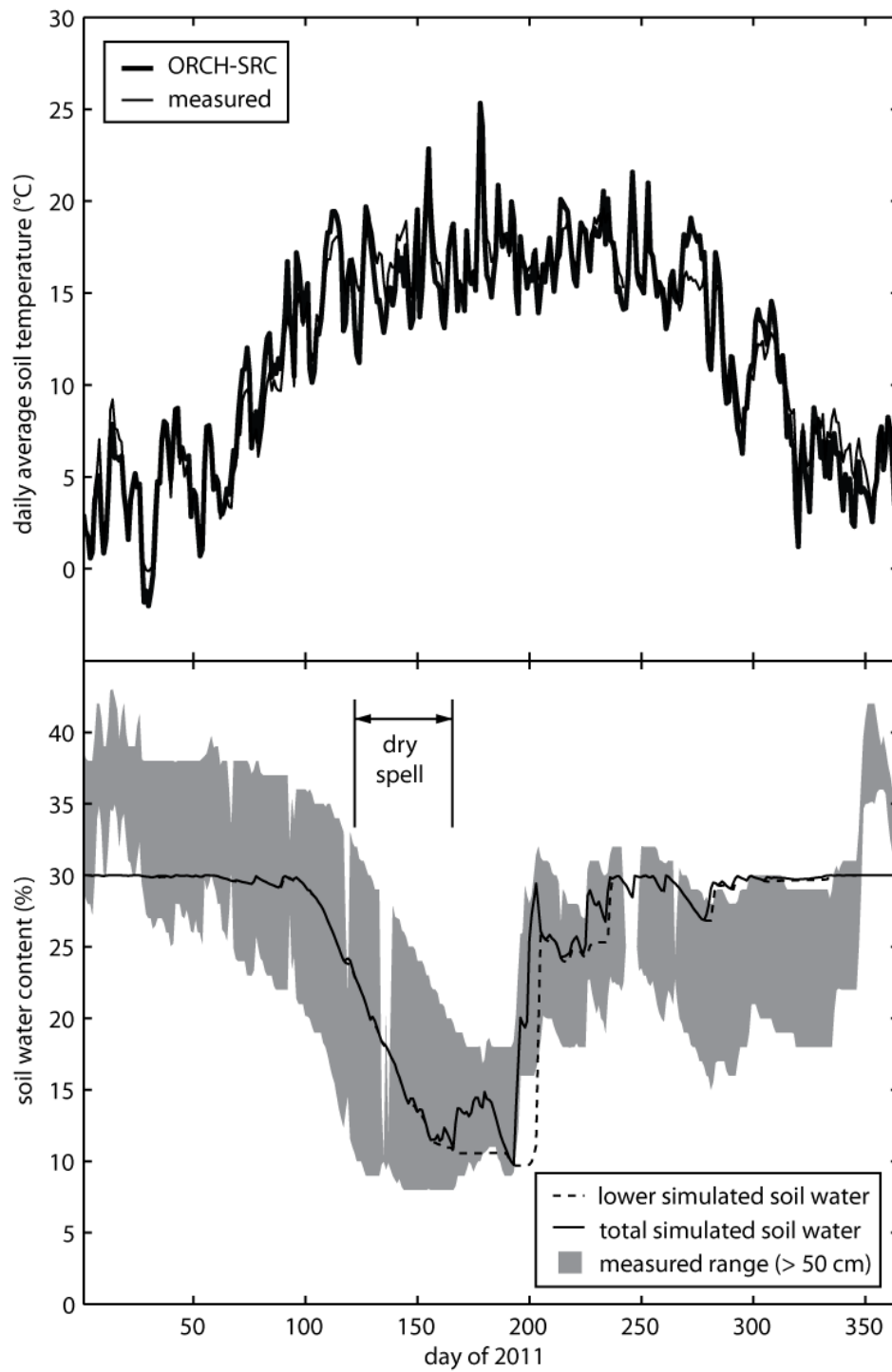
650
651

652 Fig. 5



653

654 Fig. 6



655